Wash-out processes of evaporitic sulfate salts in the Tinto river: hydrogeochemical evolution and environmental impact

C.R. Cánovas*[(1)], M. Olías[(1)], J.M. Nieto[(2)] and L. Galván[(1)].

[(1)] Department of Geodynamics and Palaeontology, University of Huelva, Campus 'El Carmen', 21071 Huelva, Spain

[(2)] Department of Geology, University of Huelva, Campus 'El Carmen', 21071 Huelva, Spain

* Corresponding author: E-mail: carlos.ruiz@dgeo.uhu.es; Fax: +34 95 921 9440

Abstract

This work deals with the wash-out processes of evaporitic salts in the Tinto river in October 2005, with the arrival of the first rainfall after the summer. In order to monitor water levels and electrical conductivity, a datalogger was set up in the river, while sampling was performed by a portable autosampler. Thirty-two samples were selected for analysis for a wide range of elements by ICP-AES. Three different flood events, with a maximum discharge of 8.1 m^3/s, were monitored. River waters suffered from a dilution effect at the beginning of the first event, recording a concentration decrease of most elements, just before the wash-out of soluble salts precipitated during the summer took place. Wash-out processes provoked a sharp increase in most element concentrations coinciding with an intense decrease in Na and Sr. After the first event, there was strong enrichment of As, and to a lesser extent in Fe, Cr and Pb, due probably to the redissolution/transformation of Fe oxyhydroxysulfates. During the third event, evaporitic sulfate salts were depleted from riverbanks ending wash-out processes, and a decrease in most element concentrations was observed. Barium exhibited different behaviour to the rest of elements owing to the solubility control exerted by barite. Lead also showed a different pattern throughout the study period, its concentration decreasing due probably to its great affinity for coprecipitate on jarosite-group minerals, and increasing when schwertmannite precipitation is thermodynamically favoured. In October 2005 the Tinto river carried around 8100 t SO_4, 1300 t Fe, 400 t Al, 100 t Zn and Cu, etc., highlighting the importance of wash-out processes of soluble salts in the Ría de Huelva ecosystem and metal fluxes into the Atlantic Ocean.

1. Introduction

The Tinto river drains one of the largest polymetallic massive sulfide regions in the world, the Iberian Pyrite Belt (IPB), which hosted original reserves of the order of 1700 million tonnes, divided up into more than 50 massive sulfide deposits, being the Riotinto Mining District (Fig. 1) the largest sulfide deposit described in the world (Sáez et al., 1999). As a consequence of sulfide oxidation processes in the IPB, the Tinto river is strongly polluted, showing extremely low pH values and high metal and SO_4 concentrations up to its confluence with the Atlantic Ocean (Cánovas et al., 2007). As a result, an enormous dissolved metal load (5075 t/a Fe, 1224 t/a Al, 687 t/a Zn, 469 t/a Cu, etc.; Olías et al., 2006) is drained into the "Ría of Huelva" estuary (Fig. 1). The adjacent Odiel river also shows a high degree of pollution from mining activities in the

IPB (Sarmiento et al., 2009) worsening the environmental quality of the "Ría of Huelva" estuary.

The existence of jarosite-rich gossans capping the pyritic ores in Riotinto indicates that acid weathering of outcropping sulfide ores could have produced natural acid rock drainage (ARD) prior to any mining activity (Lottermosser, 2003). Mining started in the 3rd Millennium B.C (Nocete et al., 2005), being intense during the Roman Period and, especially, in the 19-20th centuries (Morral, 1990). Mining activities encourage a dramatic rise in the rate of sulfide oxidation processes through promoting air accessibility and increasing surface areas of sulfides in mine workings (Nordstrom and Alpers, 1999). Therefore mining must be considered the main reason for the long-standing pollution of the Tinto river, through acid mine drainage (AMD) processes. The intensity of mining activities which took place in the IPB becomes patently obvious with a legacy of around 200 x 10^6 m^3 of wastes in the area (Sainz et al., 2004), distributed around more than 100 derelict mines. The acid leacheates coming from these AMD sources will maintain the pollution in the Tinto waters for a long time to come.

1.1. Acid Mine Drainage Processes

Acid Mine Drainage (AMD) is one of the most important water pollutant processes in the world. This process originates from the oxidation of sulfide minerals, mainly pyrite (FeS_2), the most abundant sulfide in nature. These minerals are stable in anoxic environments, however oxidation of sulfides occurs when they are exposed to atmospheric conditions, releasing acidity, SO_4 and Fe as the following overall reaction states (Nordstrom and Alpers, 1999):

$$FeS_2 + 7/2\ O_2 + H_2O \rightarrow Fe^{2+} + 2\ SO_4^{2-} + 2\ H^+ \qquad \text{Eq. 1}$$

Sulfide oxidation processes also imply release of metals (e.g., Cu, Zn, Cd, Ni.) and metalloids (e.g., As, Sb) contained in sulfides as accessory elements. The acidic leachates react with the surrounding mineral matrix releasing other elements such as Al, Ca, Si, Na, K, Mn, etc. As AMD water travels from its sources, Fe(II) is oxidised (Eq. 2) and subsequently the Fe(III) can also oxidise sulfide minerals (Eq. 3) or precipitate as Fe secondary minerals (idealized as $Fe(OH)_3$; Eq. 4).

$$Fe^{2+} + ¼\ O_2 + H^+ \rightarrow\ Fe^{3+} + ½\ H_2O \qquad \text{Eq. 2}$$

$$FeS_2 + 14Fe^{3+} + 8H_2O \rightarrow 15Fe^{2+} + 2\ SO_4^{2-} + 16H^+ \qquad \text{Eq. 3}$$

$$Fe^{3+} + 3H_2O \rightarrow Fe(OH)_3 + 3H^+ \qquad \text{Eq. 4}$$

The formation and solubility of secondary minerals have great environmental implications. The precipitation of insoluble secondary minerals with large surface areas becomes a sink for metals in acid mine water systems through adsorption and

coprecipitation processes, attenuating metal pollution. Sanchez-España et al. (2005) indicate removal rates, through retention in Fe and Al precipitating mineral phases, of around 99% of As and Fe released from AMD sources in the adjacent Odiel catchment and lower rates (60-80%) for Al, Mn, Cu, Zn, Pb and SO_4. In the Tinto river, attenuation by adsorption and coprecipitation are less important, dilution being the main mechanism responsible for metal concentration decrease downstream from AMD sources (Cánovas, 2009), due to the constant and vast inputs of low pH and Fe-rich waters from the Riotinto Mining District, maintaining a pH <3 up to its mouth in the estuary (Cánovas et al., 2007).

Soluble secondary minerals also slow down metal pollution in AMD systems (Nordstrom and Alpers, 1999), but only temporarily until the arrival of rainfall, when they are redissolved. Evaporitic sulfate salts are considered the most soluble secondary minerals in AMD systems (Blowes and Jambor, 1994). These salts can precipitate directly on mineral surface from sulfide oxidation or indirectly by evaporative processes, when mineral saturation is achieved in concentrated acid mine waters.

The mineralogy of these sulfate salts depends on the chemical composition, Eh and pH of precipitating solutions (Buckby et al., 2003). Iron(II) sulfates such as those belonging to the melanterite group (Eq. 5) prevail close to sulfide oxidation environments, from Fe(II) and very low pH (1-2) waters. Mixed Fe(II)-Fe(III) and Fe(III)-Al sulfates, mainly copiapite group members (Eq. 6), are ubiquitous on the banks of AMD-affected rivers, from Fe(III) and low pH (2-4) waters (i.e. Buckby et al., 2003; Joeckel et al., 2005; Sánchez-España et al., 2007).

$$Fe^{2+} + SO_4^{2-} + 7H_2O \rightarrow Fe_2SO_4 \cdot 7H_2O \qquad \text{Eq. 5}$$

$$4Fe(OH)_3 + Fe^{2+} + 6SO_4^{2-} + 10H^+ + 10H_2O \rightarrow Fe^{2+}Fe_4^{3+}(SO_4)_6(OH)_2 \cdot 20H_2O \qquad \text{Eq. 6}$$

Iron sulfate minerals have been observed to evolve from Fe(II) to Fe(III) phases and to dehydrate with time (Jambor et al., 2000; Jerz and Rimstidt, 2003). Knowledge of the sulfate mineralogy and paragenesis at an AMD site is important because different sulfate minerals carry different trace elements and produce different amounts of acid upon dissolution (Jerz and Rimstidt, 2003).

High concentrations of trace metals and metalloids are found in evaporitic sulfate salts precipitated in the IPB (Hudson-Edwards et al., 1999; Buckby et al., 2003; Sánchez-España et al., 2005; Romero et al., 2006; Cánovas et al., 2008; among others). Table 1 shows a summary from Cánovas et al. (2008) of the composition of evaporitic sulfate salts in the Tinto river, dominated by minerals belonging to the melanterite group (e.g., melanterite, rozenite, rhomboclase, szomolnokite, pisanite) and the copiapite-coquimbite group (e.g., aluminocopiapite, ferricocopiapite, coquimbite). Buckby et al. (2003) estimated from different sulfate salt properties (density, composition, porosity and distribution) precipitation of around 200 t Cu and 150 t Zn in the Tinto catchment during

the summer. Cánovas et al. (2008) estimated redissolution of 100 t Zn and 100 t Cu during flush-out processes in October 2004 in the Tinto system.

The dissolution of these salts implies a rapid acidification and release of enormous amounts of sulfates and contaminants to the water. They are mainly transported in dissolved form up to their arrival at the Ría of Huelva estuary, where two types of mixing processes take place: pH-induced and salt-induced mixing (López-González, 2009), with most metals trapped in the sediments during the pH-induced mixing.

1.2. Objectives

Due to the high solubility of evaporitic sulfate salts, climate is an important control on mineral formation/dissolution and mobilization of metals. Rivers in semi-arid climate regions such as the Tinto river alternate between long periods of drought and short but intense rainfall events, that can provoke quick acidification and metal concentration increase.

Unfortunately, the wash out processes are scarcely documented. Most studies are limited to mine sites or small catchments (Bayless and Olyphant, 1993; Keith et al., 2001; among others.), laboratory experiments (Hammarstrom *et al,* 2005) or focused on mineral formation (Buckby et al., 2003; Jamieson et al., 2005; Joeckel et al., 2005; Romero et al., 2006; among others.). However, little research has been carried out on wash-out processes in rivers affected by AMD, and their role in metal cycling on these environments. The main objectives of the present study are: i) to study the effects of wash-out processes of evaporitic soluble salts on the Tinto River hydrochemistry and ii) to estimate the contaminant fluxes to the Ría of Huelva.

2. Methodology

2.1. Sampling

The sampling site was located at the stream-gauge station of Gadea (Fig. 1), belonging to the Andalusian Water Agency. This point is located approximately 41 km downstream of the Riotinto Mining District and around 20 km upstream of its entry into the Ría of Huelva estuary (Fig. 1).

Sampling was carried out by a Teledyne ISCO® autosampler, with a sample container holding up to 24 bottles and an outlet pipe made of polyethylene. The inlet pipe was located approximately 2 m from the riverbank. Samples were pumped by a peristaltic pump, with a schedule purge stage between samples to avoid cross-contamination. Sample-containing bottles were washed in 10% (v/v) HNO_3 and then with milli-Q water (18.2 MΩ) prior to sampling. The sampling period comprised from 5th October to 4th November with a frequency of 2, 4 or 6 h depending on the weather forecast. Samples were filtered through 0.45 μm Millipore® teflon filters, which implies some colloidal

particles with lower diameter are considered as dissolved. Samples were subsequent acidified with suprapure HNO_3 Merk® to pH<2 and stored in the dark at 4 ºC until analysis.

Electrical conductivity (EC), temperature and water level were monitored every 10 min during the sampling period by means of a Van Essen® Diver datalogger set up at the sampling point. The CTD Diver Datalogger (DI 261) is equipped with pressure and temperature sensors and, in addition, a 4-electrode sensor to measure EC. The air pressure was compensated by means of a Barodiver Datalogger (DI 250). Corrected values from specific EC and water level were obtained.

Temperature, pH, Eh and EC of samples were measured in the field with portable meters (Hanna Instruments HI 9025 and HI 9033). The instruments were calibrated before carrying out samplings. Eh values were corrected to obtain the potential referred to the H electrode (Nordstrom and Wilde, 1998). EC values recorded by the datalogger showed a high correlation ($r^2 = 0.97$) with those taken manually. Rainfall data were obtained from 10 different gauges distributed within the Tinto catchment (Fig. 1) and water discharge was calculated from water level and the rating curve of the stream gauge station.

2.2. Analysis

From all samples taken in the monitored period, 32 were selected for analysis. The selecting criterion was significant changes in physico-chemical parameters. The chemical analysis was undertaken at the Central Research Services of the Huelva University following a custom-designed protocol specific to waters affected by AMD (Ruiz et al., 2003). Cations were analysed using Inductively Coupled Plasma Optical Emission Spectroscopy (ICP-AES) on a Jobin Yvon (JY ULTIMA 2) spectrometer. Aluminium, As, Ba, Be, Ca, Cd, Co, Cr, Cu, Fe, K, Li, Mg, Mn, Na, Ni, P, Pb, S, Si, Sr and Zn were determined, although in this work only the most significant are presented. Triplicate analyses were performed in order to evaluate the analytical precision, giving below 5% in all cases. In each analysis sequence, blanks were analysed, all elements being below the detection limit of the equipment (Table 2). The analytical accuracy was checked by the analysis of reference materials (NIST-1640).

A speciation analysis was carried out using the PHREEQC code (Parkhurst and Appello, 1999). All thermodynamics constants were taken from the geochemical WATEQ4F (Ball and Nordstrom, 1991) and MINTEQA2 (Allison et al., 1991) databases. The equilibrium constants (Ke) of schwertmannite were obtained from those provided by Bigham et al. (1996b) and Yu et al. (1999).

3. Results

3.1. Hydrochemical Variations

Before the controlled period, the Tinto river discharge decreased progressively from 0.7 in May to around 0.1 m^3/s at the end of the dry period. The water showed EC values close to 5.0 mS/cm, a pH of 2.25 and high SO_4 and metal concentrations (e.g., 356 mg/L Fe, 145 mg/L Al, 35 mg/L Zn).

The first rainfall after the summer was recorded in October, around 124 mm from the 5th October to 4th November (19% of rainfall recorded in 2005/06). Figure 2 shows the hyetograph and the hydrograph during the controlled period. Table 2 shows the basic statistics of element concentrations and physico-chemical parameters for the analyzed samples.

Three different flood events can be distinguished. Rainfall recorded from the 8th to 12th October (with maximum values of 29 and 14 mm on 11th and 12th) gave rise to Event 1 (Fig. 2), reaching a maximum discharge of 8.1 m^3/s. During this flood event a slight decrease in EC (from 4.54 to 3.36 mS/cm; Fig. 3) and an increase of pH (from 2.25 to 2.40: Fig. 3) were observed. However, immediately after, EC increased notably (maximum value of 8.04 mS/cm, 12 h after the discharge peak) while pH decreased slightly (from 2.40 to 2.24; Fig. 3). During the falling limb of the hydrograph, EC decreased progressively (Fig. 3), slightly lower values being recorded at the end of the event than at the beginning.

Less intense rainfall recorded from the 21st to 23rd October (Fig. 2) gave rise to Event 2, characterized by a maximum discharge of 4.01 m^3/s and scarce variations of EC (Fig. 3). Although some samples were taken during this event, they were not analysed due to the scarce variations in physico-chemical parameters.

Rainfall recorded from the 26th to 30th October (40 mm) gave rise to Event 3 (Fig. 2), with a maximum discharge of 6.8 m^3/s, registered on the 31st. Firstly, EC increased slightly up to a maximum value of 4.9 mS/cm, decreasing afterwards to 2.7 mS/cm, around 9 h after the discharge peak (Fig. 3). Despite a subsequent and slight EC recovery (Fig. 3), values kept on decreasing to 2.1 mS/cm at the end of Event 3. A slight decrease of pH values at the beginning of this event gave way to a quick increase up to values close to 2.55 almost 9 h after the discharge peak. At the end of the event values close to 2.65 were reached (Fig. 3).

In relation to element evolution through the monitored period, an initial decrease in concentration of most elements was recorded at the beginning of Event 1 (from 296 to 198 mg/L Fe, from 2785 to 1964 mg/L SO_4, from 124 to 88 mg/L Al.; Figs 4 and 5). Afterwards, element concentrations increased dramatically, reaching their highest values of the year (Cánovas, 2009), with maximum values of 1280 mg/L Fe, 8669 mg/L SO_4, 462 mg/L Al, etc. (Figs 4 and 5).

Sodium and Sr decreased in concentration coincident with the rise of EC values (Fig. 5). Concentrations of K fluctuated during Event 1, showing anomalous behaviour with a

decrease after the discharge peak. Barium concentrations also decreased during this event (Fig. 5).

No significant changes in EC, and therefore in the concentration of most elements, were observed between Event 1 and 3. However, a sharp increase in As concentration (Fig. 4), and to a lesser extent in Fe, Cr and Pb (Figs 4 and 5) took place.

An initial increase in most element concentrations was recorded at the beginning of Event 3, although of less importance than the increase recorded in Event 1, except for Cr (Fig. 5). Other elements such as Pb (Fig. 4) and K (Fig. 5) decreased in concentration coinciding with the increase in water mineralization. In relation to As, its concentration decreased drastically up to the end of the event (Fig. 4).

A progressive decrease in most element concentrations was subsequently recorded, reaching lower values than before the start of the controlled period (Figs 4 and 5). During Event 3 a slight recovery of most element concentrations (and EC values) was also observed after the discharge peak (samples 28 and 29), as in Event 1.

Furthermore, Pb and Ba concentrations increased coinciding with a decrease in SO_4, reaching their highest values at the end of Event 3 (Figs 4 and 5).

3.2. Saturation indices and speciation

Iron is mostly found as Fe(III) (85-100% of total Fe) due to the high Eh values recorded (between 735 and 892 mV; Table 2) in the Tinto river. The high SO_4 concentration in the Tinto river determines the formation of metal- SO_4 complexes (Fig. 6). Significant differences in speciation are predicted by PHREEQC depending on metal valences. On the one hand, trivalent cations such as Fe(III) and Al are largely found (80-90%) as metal-SO_4 complexes ($FeSO_4^+$, $Fe(SO_4)_2^-$, $AlSO_4^+$, $Al(SO_4)_2^-$), while divalent cations such as Cu, Zn, Mn, Ni, Ca, Mg, etc., are mainly found (60-70%) as individual free cations, except Ba and Pb which show a higher proportion (57-62%) of metal-SO_4 complexes ($BaSO_4$, $Ba(SO_4)_2^{2-}$, $PbSO_4$, $Pb(SO_4)_2^{2-}$). On the other hand, monovalent cations such as K, Li and Na are almost exclusively (> 97%) found as individual free cations.

In relation to the solubility of AMD-related mineral phases, Pb-jarosite and K-jarosite were supersaturated at the beginning of Event 1, while other mineral phases such as H-jarosite, Na-jarosite and schwertmannite (Fig. 7) were subsaturated. However, owing to the rise in pH and in Fe^{3+} and SO_4^{2-} activities which took place during Event 1, saturation indices (SI) of these mineral phases increased, especially schwertmannite, reaching oversaturated conditions according to the equilibrium constant provided by Yu et al. (1999).

During Event 3, the SI of jarositic minerals kept constant, whereas an increase of schwertmannite values is observed, also reaching oversaturated conditions according to the Ke provided by Bigham et al. (1996b).

Such low pH values recorded during the controlled period (2.23-2.64) cause Al to have conservative behaviour, therefore the most common AMD-related Al mineral phases such as alunite and amorphous $Al(OH)_3$ were undersaturated (Fig. 7). Only jurbanite showed SI values close to equilibrium, although it seems evident that there was a lack of Al solubility control by this mineral phase, but rather an apparent thermodynamic stability (Nordstrom and Alpers, 1999; Bigham and Nordstrom, 2000; Blowes et al., 2004).

Regarding sulfates, barite is close to saturation or even slightly oversaturated (Fig. 7) indicating a solubility control of Ba by this mineral phase. Other sulfates such as gypsum, anglesite, celestine and epsomite are undersaturated, although their SI values increased during Event 1 and to a lesser extent during Event 3 (Fig. 7), coinciding with an increase in SO_4 concentration. Throughout the monitored period, a general and slight increase in anglesite SI values was observed, meanwhile gypsum, celestine and epsomite SI values decreased.

4. Discussion

4.1. Ionic Ratios

The significant increase in concentration of most elements recorded in Event 1 is due to wash-out of evaporitic sulfate salts precipitated during summer along the Tinto catchment. The lag between the onset of rainfall and the increase of pollutant concentrations, around 5 days, seems to indicate that dissolution of soluble salts from the mining area rather than those precipitated in the surroundings, is responsible for this increase in pollutant concentrations.

During the summer a decrease in the Fe/SO_4 ratios in the Tinto river waters is recorded as a consequence of precipitation of Fe mineral phases (Cánovas et al., 2007), up to a value of 0.12 before the controlled period (Table 3). The Fe/SO_4 ratio in sulfate salts precipitated along the catchment is higher (0.25; Table 3), therefore dissolution of these soluble salts causes a rise of this ratio in river water during the discharge peak in Event 1 (Fig. 8). For the same reason, an increase in Fe/Al ratios and decreases in Fe/As, Co/Pb and Ca/Mg ratios were observed (Fig. 8 and Table 3).

Values of Cu/Zn ratios in evaporitic sulfate salts are quite similar to those found in Tinto waters during the summer (Table 3). Therefore, Cu/Zn ratios scarcely change during the monitored period (Fig. 8).

Between Event 1 and Event 3, increases in Fe/SO_4 and Fe/Al ratios coinciding with a decrease in Co/Pb and Fe/As ratios were observed, owing to the sharp increase in As concentration and to a lesser extent, in Fe and Pb. During Event 3, Fe concentration decreased in relation to As and Al due to the progressive wash-out of soluble salts along the catchment.

4.2. Principal Component Analysis (PCA)

A principal component analysis (PCA) of the results has been carried out to study relationships among variables. As some variables do not show a normal distribution, Spearman's correlation matrix has been used for the PCA (Davis, 1986).

During Event 1, the first component describes 68% of the sample variance (Fig. 9.I) and it is related to water mineralization. Most variables (discharge, SO_4, Al, Co, Cd, Cr, etc.) are located in the positive side of component 1, meanwhile pH is placed in the negative part as pH values increase when the concentration of most elements decreases.

The second component explains a much lower percentage of variance (21%) and on its positive side are located: Na, Sr, Si, Li, Ca and Ba (Fig. 9.I), together with Eh. Other variables such as pH, K and As are placed in the negative side. This component seems to be related to lithological factors. During summer, Tinto river waters show high concentrations of Na, Sr, Ca, etc., due to the longer interaction of the acidic waters with the marly materials belonging to the Miocene, which outcrop in the lowest reach of the river (Cánovas et al., 2007). On the other hand, during summer As concentration is very low owing to the intense precipitation of oxyhydroxysulfates, which favours intense As adsorption/coprecipitation processes (Cánovas et al., 2007). The location of K in Fig. 9 I, close to pH and As (in relation to the second component of the PCA) seems to indicate K-jarosite precipitation during Event 1.

The PCA of samples (Fig. 9.II) indicates a decrease in Na and Sr concentration (component 2) and a slight drop of EC and rise of pH values between samples 1 and 6 (process A). This may be due to the arrival of less mineralized waters, as the decrease in Na and Sr is greater due to their high concentration in the river water during summer. At the same time, redissolution of sulfate salts precipitated in the surroundings can take place. However, wash-out processes are not so intense as to offset the dilution effect caused by less mineralised runoff waters, the reason why a slight decrease in EC values and in concentrations of SO_4, Fe, Al, etc., are observed.

Sample 7 coincides with the highest discharge value recorded during Event 1, although the highest concentrations are found in sample 8 at the beginning of the falling limb (Fig. 9.II). Waters suffer from an enrichment in most elements (Fig. 9.II) due to the redissolution of evaporitic sulfate salts (process B). An enrichment in elements linked to component 2 is not observed (Na, Sr, etc.) as soluble salts precipitated in the Tinto river usually show low Na concentrations (Table 3). Although the Sr/SO_4 ratio has not been documented in precipitating salts in the Tinto river, low values of this ratio were found in sulfate salts by Bayless and Olyphant (1993).

Samples from 8 to 19 correspond to the falling limb of Event 1 (Fig. 9.II), the mineralization of water diminishes progressively while pH values increase, once the wash-out of soluble salts is less important and the arrival of runoff waters decreases

(process C). Potassium is the only element which increases in concentration during this stage. This tendency seems to be reversed in samples 13 and 14 (Fig. 9.II), coinciding with a slight recovery in most element concentrations (Figs 4 and 5) during the falling limb.

Samples from Event 2 were not analyzed due to the scarce variations in EC, despite the rise in discharge. The redissolution of soluble salts during this event must have been partially counteracted by the dilution effect of low-mineralization runoff waters.

In relation to Event 3, the first component (Fig. 9.III) explains most of the sample variance (85%), and it is related, as in Event 1, to sample mineralization. Barium, K, Pb and pH are located in the negative side of component 1. It is striking that Pb was located in the positive side of this component during Event 1. The second component (Fig. 9.III) describes a much lower percentage of variance (6%) and is mainly related to discharge and, to a lesser extent, to Pb and Ba.

The PCA of samples during Event 3 (Fig. 9.IV) indicates a progressive increase in discharge and in most element concentrations (process D) with the onset of rainfall (less intense but more continuous than in Event 1), due to a new process of redissolution of soluble salts (samples 20 to 23).

Afterwards, at increasing discharge a decrease in concentration of most elements is observed, coinciding with an increase of pH values and in K, Pb and Ba concentration (process E, samples 24 and 25). This indicates the end of wash-out processes of evaporitic sulfate salts stored during summer, which were being progressively dissolved until this time.

During the falling limb, pH, Ba, Pb and K increase in value coinciding with a drop in concentration of Fe, SO_4, Al, Ca, etc., (samples 26 to 32, process F) in such a way that concentrations at the end of the controlled period are lower than at the beginning, except for Ba, K and Pb.

As in samples 13 and 14 of Event 1 a recovery in most element concentrations is recorded in Event 3 (samples 28 and 29). This seems to indicate the influence of AMD-affected waters coming from the Riotinto Mining District (Fig. 1) with a lower response time to rainfall.

4.3. Discharge-Concentration (Q-C) relationships

Two opposing processes determine Q-C relationships during the events (Fig. 10): (1) the increase of water mineralization resulting from the wash-out of soluble evaporitic salts precipitated during summer and (2) the decrease of water mineralization due to dilution by runoff waters. These processes were also inferred from PCA (Fig. 9). Competition between these processes can give rise to two types of hysteresis curves (Evans and Davies, 1998). For SO_4 in Event 1, an initial dilution can be observed (up to sample 6), followed

by a sharp increase in concentration. For the same discharge, much higher SO_4 values occur in the falling than in the rising limb, i.e. maximum concentration is after maximum discharge. The occurrence of this type of hysteresis is known as counter clockwise loop, characterized by an initial dilution for low-mineralised runoff waters, followed by an increase in EC values for highly-mineralised water coming from the wash-out of soluble salts in the farther points of the catchment.

In Event 3, lower SO_4 concentrations occur in the falling than in the rising limb, i.e. maximum concentration (sample no. 23) is before maximum discharge, recording an inverse hysteresis process known as *clockwise loop*. This type of hysteresis occurs when all soluble salts stored during the summer are consumed before maximum discharge and the dilution effect of low-mineralised runoff waters is the process controlling the Q-C relationship. Also in Figure 10, the arrival of highly mineralised waters during the falling limb of both Event 1 (samples 13 and 14) and Event 3 (samples 28 and 29) can be observed, as mentioned previously in section 3.1.

The evolution of As in Figure 10 is quite similar to SO_4 during Event 1, although a huge increase in As concentration is subsequently observed despite the lack of discharge variations (samples 17 to 20). This enrichment was also noted, although to a lesser extent, for Fe, Pb and Cr. This process has previously been described by Cánovas et al. (2008) in October 2004. Elements such as Pb, Cr and As have a strong affinity to coprecipitate and/or adsorb onto Fe oxyhydroxysulfates. The increase observed between Events 1 and 3 could be due to initial oxyhydroxysulfates (jarosites or schwertmannite) precipitating during the discharge peak in Event 1 retaining these elements, followed by a subsequent release through desorption or transformation processes of these mineral phases, increasing the concentration of Fe, Pb, Cr and especially of As. In fact, during the discharge peak in Event 1, an increase in SI of these mineral phases is recorded (Fig. 7). The switch of As(V) aqueous speciation from $H_3AsO_4^0$ to $H_2AsO_4^-$ at a pH of around 2.5 would promote desorption processes and could also contribute to the increase of dissolved As concentration (Dixit and Hearing, 2003). Nevertheless, an in-depth study on this subject needs to be conducted in future work. In relation to Event 3, the evolution of As concentration relative to discharge is similar to that found for SO_4 (Fig. 10), although similar concentrations of As are found at the start and end of the controlled period.

Sodium displays a totally different Q-C plot (Fig. 10). During the rise in discharge in the first Event, Na concentration drops owing to the high values found in river water after summer and the low Na content in both sulfate salts and runoff waters, commented on previously. This decrease in Na concentration remains during the falling limb. During Event 3, Na evolution is not discharge dependant as runoff waters have a similar Na concentration to the Tinto river waters.

In the Q-C plot for Pb (Fig. 10) similar behaviour to SO_4 and As can be seen during Event 1. An increase in Pb concentration is recorded between Event 1 and 3, although not so intense as that for As. During Event 3, Pb concentration increases coinciding with a rise in discharge, reaching its highest values during the falling limb of the hydrograph. This behaviour will be explained in the next section.

4.4. Solubility controls of Pb

As was inferred from the PCA and Q-C relationship, Pb shows different behaviour during Event 1 and 3. Lead shows similar behaviour to SO_4 and most elements during Event 1, while during Event 3 its behaviour is linked to Ba, K and pH. This could be due to the occurrence of two different solubility controls. The first one seems to be related to the affinity of Pb to coprecipitate and be adsorbed by jarositic minerals (Dutrizac and Jambor, 2000; Acero et al., 2006), and the second one on the control exerted by coprecipitation/adsorption on schwertmannite or precipitation of anglesite.

As was stated in section 3.2, during Event 1 all the sampled waters were oversaturated with respect to K-jarosite and Pb-jarosite and undersaturated with schwertmannite. The solubility of schwertmannite and the jarositic minerals is defined by the following overall reactions:

$$Fe_8O_8(OH)_x(SO_4)_y + (24-2y)H^+ \rightarrow 8Fe^{3+} + ySO_4^{2-} + (24-2y+x)/2\ H_2O \quad \text{Eq. 7}$$

with *y* values between 1 and 1.75 and $x = 8-2y$ (Bigham et al., 1996b).

$$MeFe_3(SO_4)_2(OH)_6 + 6H^+ \rightarrow Me^+ + 3Fe^{3+} + 2SO_4^{2-} + 6H_2O \quad \text{Eq. 8}$$

being Me in Eq. 8 Na, K, Pb or H^+.

Bigham et al. (1996a) suggest jarosite and schwertmannite precipitation in acidic and oxidising SO_4-rich waters within a pH range between 2.3 and 3.6, jarosite being the prevailing precipitating phase at low pH values. However, limits in the stability fields between jarosite and schwertmannite also depend on the activity of Fe^{3+}, SO_4^{2-} and K^+. Higher Fe^{3+}/SO_4^{2-} ratios will favour schwertmannite precipitation due to the higher Fe(III) content in its formula (Eq. 7)

Lead seems to be more strongly adsorbed/coprecipitated by jarosite than by schwertmannite because this element fills the structural sites of K^+, Na^+ and H^+ in jarosite (Dutrizac and Jambor, 2000). Acero et al. (2006) documented, from schwertmannite ageing experiments, a decrease in Pb concentration during H_3O-jarosite precipitation. This suggests that jarosite coprecipitation can play a key role in Pb behaviour in AMD waters.

The rise in pH and in Fe/SO_4 ratio recorded through the monitored period would favour schwertmannite precipitation over jarosite during Event 3. That is, schwertmannite precipitation at the end of the controlled period could provoke the increase in Pb concentration as it is no longer coprecipitated/adsorbed by jarosite. Precipitation of

schwertmannite would also explain the decrease in As concentration recorded at the beginning of Event 3 (Fig. 4). The increase in K concentration in this period also supports this hypothesis, since K would not be removed by jarosite precipitation.

Considering equilibrium reactions of jarosite and schwertmannite, provided by Chapman et al. (1983) and Yu et al. (1999), respectively:

$KFe_3(SO4)_2(OH)_6 + 6H^+ \Leftrightarrow K^+ + 3Fe^{3+} + 2SO_4^{2-} + 6H_2O$ $\quad logK_J = -9.21$ Eq.9

$8Fe^{3+} + 1.8SO_4^{2-} + 12.4H_2O \Leftrightarrow Fe_8O_8(OH)_{4.4}(SO_4)_{1.8} + 20.4H^+$ $\quad logK_S = -10.5$ Eq.10

The following equilibrium reaction can be established between both mineral phases:

$KFe_3(SO4)_2(OH)_6 + 5\ Fe^{3+} + 6.4H_2O \Leftrightarrow$

$Fe_8O_8(OH)_{4.4}(SO4)_{1.8} + K^+ + 0.2SO_4^{2-} + 14.4H^+$ $\quad logK_{JS} = -19.71$ Eq.11

From this reaction the pH value at which both mineral phases coexist can be obtained:

$$pH_{JS} = \frac{0.2\log(SO_4^{2-}) + \log(K^+) - 5\log(Fe^{3+})}{14.4} + 1.37 \qquad \text{Eq.12}$$

Figure 11 depicts the equilibrium of K-jarosite and schwertmannite (solid line) and samples (circles) as a function of pH and activities of Fe^{3+}, K^+ and SO_4^{2-} according to Equation 12. The dashed lines indicate the limits between both minerals considering the solubility window for schwertmannite (log K_{JS} = -19.71 ±2.5) proposed by Yu *et al.* (1999). The increase in Pb concentration can be clearly seen when samples are located in the schwertmannite stability field.

The pattern of the samples in Figure 12 seems to indicate a solubility control by anglesite during the third event, although the samples are slightly undersaturated. It can be seen that when SO_4^{2-} activity decreases Pb activity increases almost in a parallel direction to the saturation line. The samples are slightly subsaturated in anglesite (next to saturation line SI=-1), which could indicate that simultaneously a coprecipitation/adsorption process onto schwertmannite occurs.

4.5. Environmental Implications

The metal load carried by the Tinto river during Event 1 and the whole controlled period has been estimated by means of the following expression:

$$L_T = \Sigma\ ½\ (C_{i\ (n)} + C_{i\ (n+1)})\ Q_{T\ (n \rightarrow n+1)} \qquad \text{Eq. 13}$$

where L_T is the total load, C_i the pollutant concentration in sample i and Q_T the discharge.

On the other hand, from the EC values recorded by the datalogger, the pollutant load of those elements showing a good correlation ($R^2 > 0.80$) with EC can be estimated (Table 4). For these elements this implies a higher accuracy in the estimation, as samples between Event 1 and Event 3 were not analyzed. Correlations between EC and concentration with $R^2 > 0.80$ were established for most elements, except for Fe, As, Cr and Pb.

Estimations obtained from Eq. 13 show a pollutant load during Event 1 of 3754 t SO_4, 550 t Fe, 193 t Al, etc. (Table 4). In spite of the higher average discharge during Event 3, most sulfate salts have been previously washed out and the pollutant load carried by the Tinto river is lower than in Event 1 for most pollutants (2323 t SO_4, 400 t Fe, 110 t Al etc.). Only As and Pb were transported in higher amounts by the Tinto river during Event 3.

These values are similar to those obtained from relationships between discharge and element concentrations (Table 4) which supports the results obtained. For the whole period, values of around 8100 t SO_4, 400 t Al, 100 Zn were obtained.

Comparing these values with those estimated by Cánovas et al. (2008) in October 2004, a similar pollutant load of Al, Cu, Cd, Co, Li, Ni and Zn is observed (Table 4). The similarity between pollutant loads in both periods is striking, since different hydrological conditions were observed. The Tinto river carried around 9.2 hm^3 of water during October 2004 and only 0.91 hm^3 in October 2005 (Cánovas, 2009). However, the hydrological year 2003/04 was notably more humid (769 mm) than 2004/05 (only 307 mm), so the controlled period in October 2005 occurred after an extremely dry season. Therefore, soluble salt accumulation within the catchment was more intense during the hydrological 2004/05, owing to the slower water circulation through the catchment and the higher element concentrations in river water.

On the other hand, some differences in pollutant loads are observed between both periods. Sulfate, Fe, As and Cr loads were higher in October 2005 due to the high concentration of these elements in sulfate salts. However, the pollutant load of Pb was much higher in October 2004. This is mainly due to the only sample coinciding with discharge values close to 100 m^3/s and a high Pb content which could cause the overestimation.

Wash-out processes of evaporitic sulfate salts result in a great environmental impact on the Ría of Huelva estuary. During October 2005 the Tinto river transported around 22% and 35% of the annual pollutant load into estuary (Table 4) despite that the monthly discharge only accounted for 8.3% of the annual river contribution, showing the importance of wash-out processes on metal fluxes to the ocean under these climatic conditions. High quantities of Fe, Al and Mn are carried by the Tinto river during these processes, releasing acidity by means of hydrolysis reactions during estuarine mixing processes. This increase in mineral acidity may provoke a movement of these processes toward the outer zone of the estuary, where pH neutralisation takes place, and may increase the bioavailability of metals contained in the estuarine sediments (Nieto et al., 2007, López-González, 2009).

5. Conclusions

The analysis of the flood events recorded in October 2005 after the dry period in the Tinto river, close to its mouth, allow the following conclusions to be made.

A slight decrease in water mineralization is recorded with the onset of the first rainfall. This indicates a higher degree of dilution by runoff water over wash-out processes of soluble salts in the surroundings of the sampling point.

Once rainfall was more intense and discharge rose (up to 8 m^3/s), electrical EC values increased enormously (from 3.60 to 7.97 mS/cm) due to the arrival of leacheates generated by wash-out processes of soluble salts precipitated in the mining area. The maximum EC value was recorded 12 h after the discharge peak.

A strong decrease in concentration of Na, Sr and other elements, which showed high values during the summer, was observed. Simultaneously an increase in concentration of most elements, except for Na, Sr, Ba and K was observed. The composition of evaporitic sulfate salts explains the greater increase shown for some elements (e.g., Fe, As, Pb, Mg.) in relation to others (e.g., Al, Co, Ca.).

As a consequence of the wash out of evaporitic salts during Event 1, a counter clockwise hysteresis process occurs and, for the same discharge, the highest concentrations were reached during the falling limb.

A second flood event of less importance (4 m^3/s) was recorded, although no significant changes in EC values were observed due to the dilution effect exerted by uncontaminated runoff waters, which must counteract the wash-out process of soluble salts during this event.

During Event 3, with similar discharge values (6.8 m^3/s) to Event 1, wash-out of soluble salts carried on taking place and as a result an initial increase in most element concentrations was observed. However, once these soluble salts were depleted, most element concentrations decreased with a rise in discharge, at the end of the controlled period having lower concentrations than just after summer (clockwise type hysteresis).

Most element concentrations decreased between Event 1 and 3. On the other hand, As increased sharply, as to a lesser extent did Fe, Cr and Pb. This process must be due to redissolution/transformation of Fe oxyhydroxysulfates and/or desorption processes.

During both flood events studied, Ba shows different behaviour, its concentration increase coinciding with a decrease in SO_4 concentration due to the solubility control exerted by barite.

Lead behaves totally different between both flood events studied. During Event 1, its behaviour seems to be related to SO_4 and most elements, meanwhile during Event 3 it is linked to Ba and K. This behaviour could be associated with the precipitating oxyhydroxysulfate. Lead has a great affinity to coprecipitate on jarositic minerals. At the beginning of the controlled period, jarositic minerals are the most probable Fe oxyhydroxysulfates precipitating and the Pb concentrations were lower. As the event

progresses, pH and Fe^{3+}/SO_4^{2-} ratios increased, promoting schwertmannite as the most stable phase. This would explain the strong increase in Pb concentrations during Event 3, when anglesite controls Pb solubility, reaching its highest concentrations coinciding with the lowest values of SO_4.

During the whole controlled period, the Tinto river carried around 8100 t SO_4, 1300 t Fe, 400 t Al, etc. The pollutant loads of Al, Cu, Cd, Co, Li, Ni and Zn are quite similar to those carried by the Tinto river in October 2004, while the load of elements such as Fe, As and Cr are appreciably higher. This is striking as total discharge carried by the Tinto river in October 2005 was 10 times lower than in the same period of 2004, indicating the importance of wash-out processes of soluble salts on the metal fluxes into the estuary.

The wash-out processes of evaporitic soluble salts lead to environmental impacts on the Ría de Huelva estuary and provoke a movement of the estuarine mixing processes towards the outer zones of the estuary. This may modify the pattern of metal retention by sediments and increase the bioavailability of these metals.

Acknowledgements

This work was financed by the Spanish Ministry of Education and Science through project CTM2007-66724-C02-02/TECNO and by the Environmental Council of Andalusia. We sincerely thank two anonymous reviewers for their helpful comments on an earlier version of this manuscript. Finally, we also appreciate the review made by Dr. Ron Fuge, which helped to improve the quality of the paper.

References

Acero, P., Ayora, C., Torrento, C., Nieto, J. M., 2006. The behavior of trace elements during schwertmannite precipitation and subsequent transformation into goethite and jarosite. Geochim. Cosmochim. Acta 70, 4130-4139.

Allison, J.D., Brown, D.S., Novo-Gradac K.J., 1991. MINTEQA2/PRODEFA2, A Geochemical Assessment Model for Environmental Systems: Version 3.0 User_s Manual. Report EPA/600/3-91/021, US Environmental Protection Agency, Office of Research and Development, Environmental Research Laboratory, Athens, Georgia.

Ball, J.W., Nordstrom, D.K., 1991. User's manual for WATEQ4F, with revised thermodynamic data base and test cases for calculating speciation of major, trace, and redox elements in natural waters. U.S. Geol. Surv. Open-File Rep., 91-183.

Bayless, E.R., Olyphant, G.A., 1993. Acid-generating salts and their relationship to the chemistry of groundwater and storm runoff at an abandoned mine site in southwestern Indiana, USA. J. Contam. Hydrol. 12, 313-328.

Bigham, J.M., Nordstrom, D.K., 2000. Iron- and Aluminium-Hydroxysulfate Minerals. In: Alpers, C. N., Jambor, J. L., Nordstrom, D. K. (Eds), Sulfate Minerals - Crystallography, Geochemistry and Environmental Significance. Reviews in Mineralogy and Geochemistry 40, 351-403.

Bigham, J.M., Schwertmann, U., Phab, G., 1996a. Influence of pH on mineral speciation in a bioreactor simulating acid mine drainage. Appl. Geochem. 11, 845-849.

Bigham, J.M., Schwertmann, U., Traina, S.J., Winland. R.L., Wolf, M., 1996b. Schwertmannite and the chemical modeling of iron in acid sulfate waters. Geochim. Cosmochim. Acta 60, 2111-2121.

Blowes, D.W., Jambor, J.L. (Eds), 1994. The Environmental Geochemistry of Sulfide Mine-Wastes. Short Course Handbook 22, Mineralogical Association of Canada.

Blowes, D.W., Ptacek, C.J., Jambor, J.L., Weisener, C.G., 2004. The geochemistry of acid mine drainage. In: Lollar, B. S. (Ed.), Environmental Geochemistry (Holland, H.D., Turekian, K.K., Exec. Eds) Treatise on Geochemistry., 9, Elsevier. 149-204.

Buckby, T., Black, S., Coleman, M.L., Hodson, M.E., 2003. Fe-sulphate rich evaporative mineral precipitates from the río Tinto, southwest Spain. Mineral. Mag. 67, 263-278.

Cánovas, C.R., 2009. La calidad del agua de los ríos Tinto y Odiel. Evolución temporal y factores condicionantes de la movilidad de los metales. Ph.D Thesis. H 96-2009. http://hdl.handle.net/10272/604

Cánovas, C.R., Hubbard, C.G., Olías, M., Nieto, J.M., Black, S. Coleman, M.L., 2008. Hydrochemical variations and contaminant load in the Rio Tinto(Spain) during flood events. J. Hydrol. 350, 24-40.

Cánovas, C.R., Olias, M., Nieto, J.M., Sarmiento, A.M., Cerón, J.C., 2007. Hydrogeochemical characteristics of the Odiel and Tinto rivers (SW Spain). Factors controlling metal contents. Sci. Total Environ. 373, 363-382.

Chapman, B.M., Jones, D.R., Jung, R.F., 1983. Processes Controlling Metal-Ion Attenuation in Acid-Mine Drainage Streams. Geochim. Cosmochim. Acta 47, 1957-1973.

Davis, J.C., 1986. Stadistics and Data Analysis in Geology. John Wiley and sons. New York.

Dixit, S., Hering, J.G., 2003. Comparison of arsenic(V) and arsenic(III) sorption onto iron oxide minerals: implications for arsenic mobility. Environ. Sci. Technol. 37 18, 4182–4189.

Dutrizac, J., Jambor, J., 2000. Jarosites and their application to hydrometallurgy. In: Alpers, C.N., Jambor, J.L., Nordstrom, D.K. (Eds), Sulfate Minerals: Crystallography, Geochemistry and Environmental significance. Reviews in Mineralogy and Geochemistry 40, 405–452.

Evans, C., Davies, T.D., 1998. Causes of concentration/discharge hysteresis and its potential as a tool for analysis of episode hydrochemistry. Water Resour. Res. 34, 129–137.

Hammarstrom, J.M., Seal II, R.R., Meier, A.L., Kornfeld, J.M., 2005. Secondary sulfate minerals associated with acid drainage in the eastern US: recycling of metals and acidity in surficial environments. Chem. Geol. 215, 407-431.

Hudson-Edwards, K.A., Schell, C., Macklin, M.G., 1999. Mineralogy and geochemistry of alluvium contaminated by metal mining in the Rio Tinto area, southwest Spain. Appl. Geochem. 14, 1015-1030.

Jamieson, H.E., Robinson, C., Alpers, C.N., McCleskey, R.B., Nordstrom, D.K., Peterson, R.C., 2005. Major and trace element composition of copiapite-group minerals and coexisting water from the Richmond mine, Iron Mountain, California. Chem. Geol. 215, 387-405.

Jambor, J.L., Nordstrom, D.K., Alpers, C.N., 2000. Metal-sulfide salts from sulfide mineral oxidation. Reviews in Mineralogy and Geochemistry 40, 305-340.

Jerz, J.K., Rimstidt, J.D., 2003. Efflorescent sulfate minerals: Paragenesis, relative stability and environmental impact. Am. Mineral. 88, 1919-1932.

Joeckel, R.M., Ang Clement, B.J., VanFleet Bates, L.R., 2005. Sulfate-mineral crusts from pyrite weathering and acid rock drainage in the Dakota Formation and Graneros Shale, Jefferson County, Nebraska. Chem. Geol. 215, 433-452.

Keith, D.C., Runnells, D.D., Esposito, K.J., Chermak, J.A., Levy, D.B., Hannula, S.R., Watts, M., Hall, L., 2001. Geochemical models of the impact of acidic groundwater and evaporative sulfate salts on Boulder Creek at Iron Mountain, California. Appl. Geochem. 16, 947-961.

López-González, N., 2009. Estudio de marcadores ambientales sedimentarios y geoquímicos en los sedimentos del estuario de los ríos Tinto y Odiel. Ph.D. Thesis. Univ. Huelva.

Lottermoser, B.G., 2003. Mine Wastes. Characterization, Treatment, Environmental Impacts. Springer-Verlag, Berlin Heidelberg.

Morral, F.R., 1990 A mini-history of the Rio Tinto (Spain) region. Can. Min. Metall. Bull. 83, 150-154.

Nieto, J.M., Sarmiento, A.M., Olías, M., Cánovas, C.R., Riba, I., Kalman, J., Delvalls, T.A., 2007. Acid mine drainage pollution in the Tinto and Odiel rivers (Iberian Pyrite Belt, SW Spain) and bioavailability of the transported metals to the Huelva estuary. Environ. Internat. 33, 445-455.

Nocete, F., Alex, E., Nieto, J.M., Sáez, R., Bayona, M.R., 2005. An archaelogical approach to regional environmental pollution in the south-western Iberian Peninsula related to Third Millenium B.C mining and metallurgy. J Archaeol. Sci. 32, 1566-1576.

Nordstrom, D.K., Alpers, C.N., 1999. Geochemistry of acid mine waters. In: The environmental geochemistry of mine waters. Rev. Econ. Geol. 6A, 133-160.

Nordstrom, D.K., Wilde, F.D., 1998. Reduction–oxidation potential (electrode method). In: National field manual for the collection of water quality data, U.S. Geological Survey techniques of water-resources investigations, book 9, chapter 6.5.

Olías, M., Cánovas, C.R., Nieto, J.M., Sarmiento, A.M., 2006. Evaluation of the dissolved contaminant load transported by the Tinto and Odiel rivers (South West Spain). Appl. Geochem. 21, 1733-1749.

Parkhurst, D.L., Appelo, C.A.J., 1999. User's guide to PHREEQC- A computer program for speciation, reaction-path transport, and inverse geochemical calculations. U.S. Geol. Surv. Water Resour. Invest. Rep. 99-4259,.

Romero, A.J., González, I., Galán, E., 2006. The role of efflorescent sulfate salts in the storage of trace elements in stream waters polluted by acid mine drainage: the case of Peña del Hierro, southwestern Spain. Can Mineral. 44, 1341-1346.

Ruiz, M.J., Carrasco, R., Pérez, R., Sarmiento, AM., Nieto, J.M., 2003. Optimización del análisis de elementos mayores y traza mediante UN-ICP-OES en muestras de drenaje ácido de mina. Proc. IV Iberian Geochemical Meeting, 14-18 July. Coimbra, Portugal. Universidad de Coimbra. 402–404.

Sáez, R., Pascual, E., Toscano, M., Almodóvar, G.R., 1999. The Iberian type of volcano-sedimentary massive sulphide deposits. Mineral. Deposita 34, 549-570.

Sainz, A., Grande, J.A., de la Torre, M.L., 2004. Characterisation of heavy metal discharge into the Ria of Huelva. Environ. Internat. 30, 557-566.

Sánchez España, J., Lopez Pamo, E., Santofimia, E., Aduvire, O., Reyes, J., Barettino, D., 2005. Acid mine drainage in the Iberian Pyrite Belt (Odiel river watershed, Huelva, SW Spain): Geochemistry, mineralogy and environmental implications. Appl. Geochem. 20, 1320-1356.

Sánchez-España, J., Lopez Pamo, E., Santofimia Pastor, E., 2007. The oxidation of ferrous iron in acidic mine effluents from the Iberian Pyrite Belt (Odiel Basin, Huelva, Spain): Field and laboratory rates. J Geochem. Explor. 92, 120-132.

Sarmiento, A.M., Nieto, J.M., Olías, M., Cánovas, C.R., 2009. Hydrochemical characteristics and seasonal influence on the pollution by acid mine drainage in the Odiel river Basin (SW Spain). Appl. Geochem. 24, 697-714.

Yu, J.Y., Heo, B., Choi, I.K., Cho, J.P., Chang, H.W., 1999. Apparent solubilities of schwertmannite and ferrihydrite in natural stream waters polluted by mine drainage. Geochim. Cosmochim. Acta 63, 3407-3416.

Figure captions

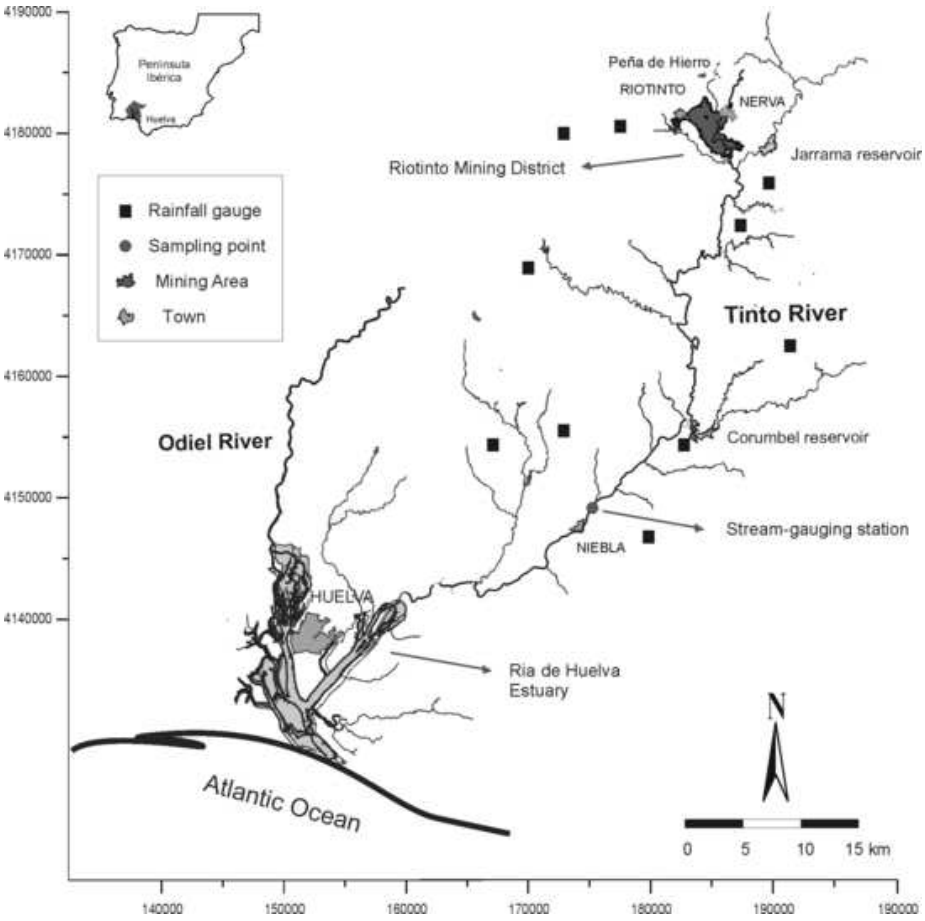

Figure 1. Map of the Tinto river showing the location of the sampling point, the mining area and the pluviometric gauges

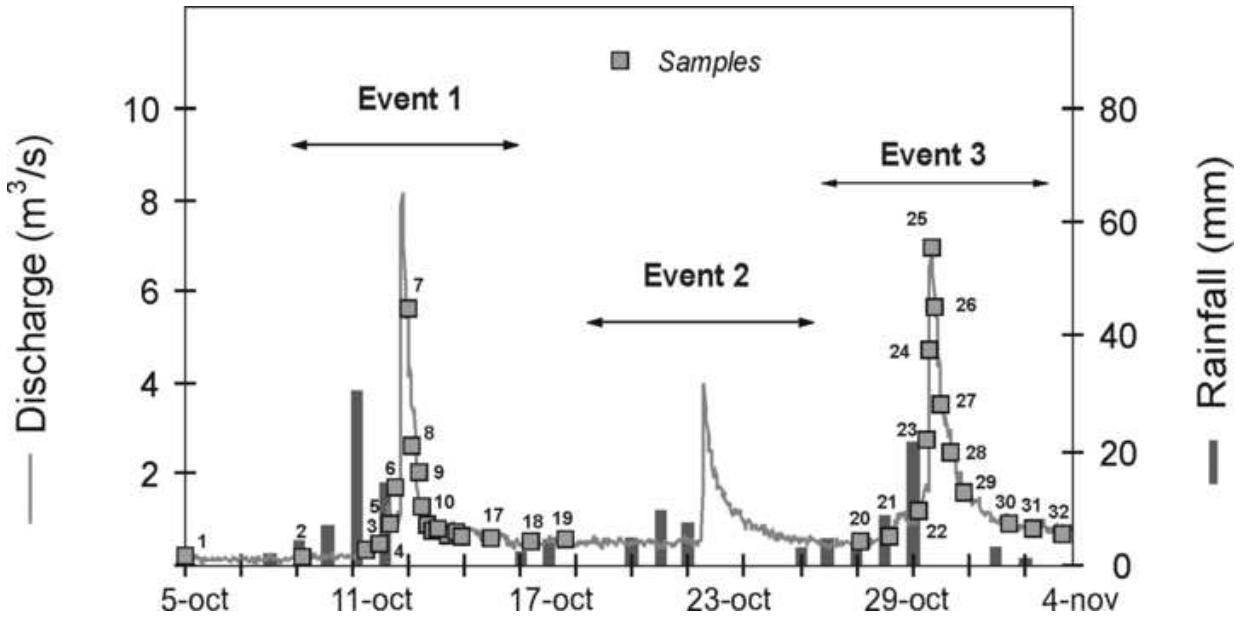

Figure 2. Hyetograph and hydrograph of Tinto river during the controlled period (indicating samples collected).

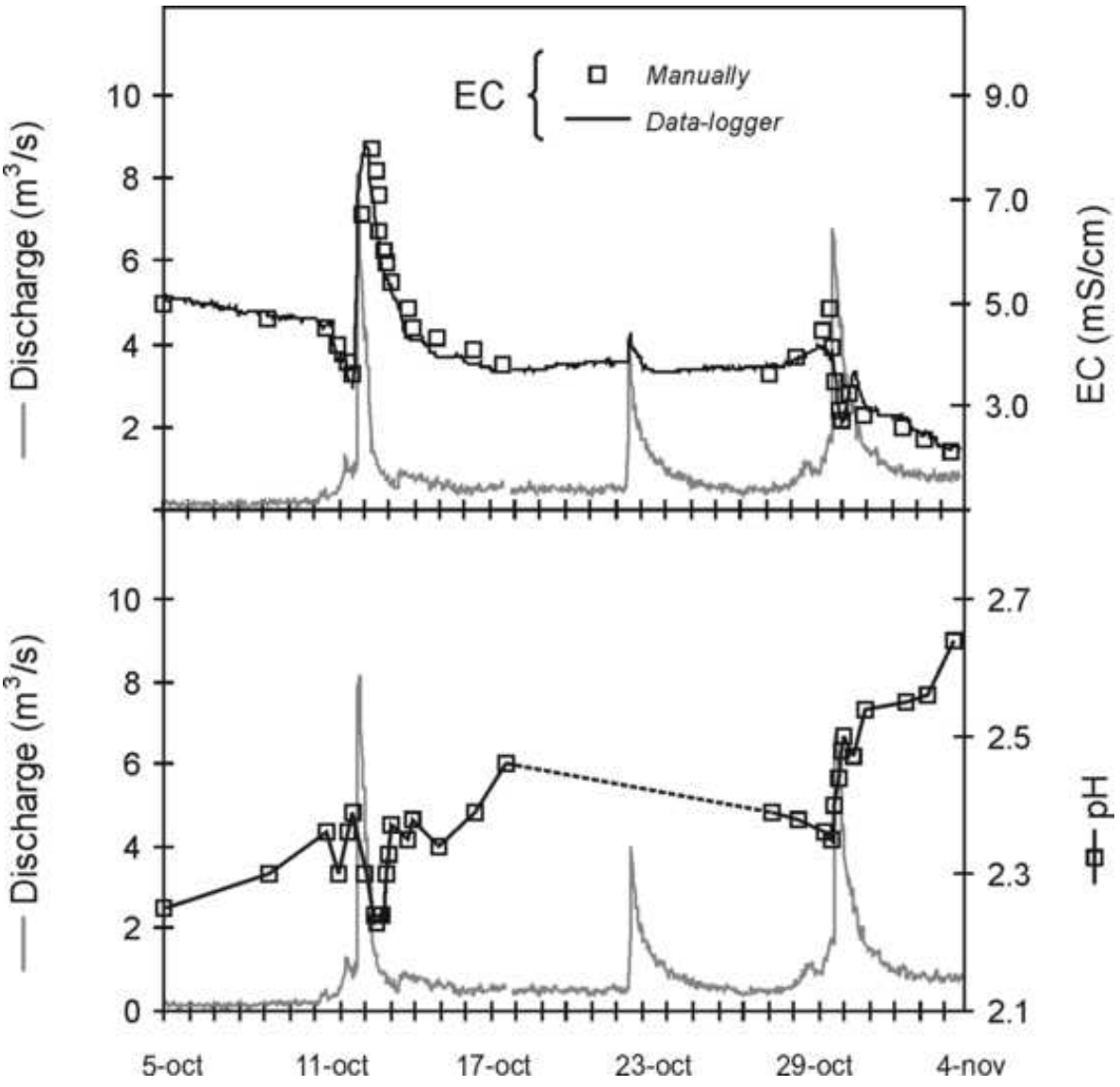

Figure 3. Electrical conductivity (EC) and pH evolution through the controlled period.

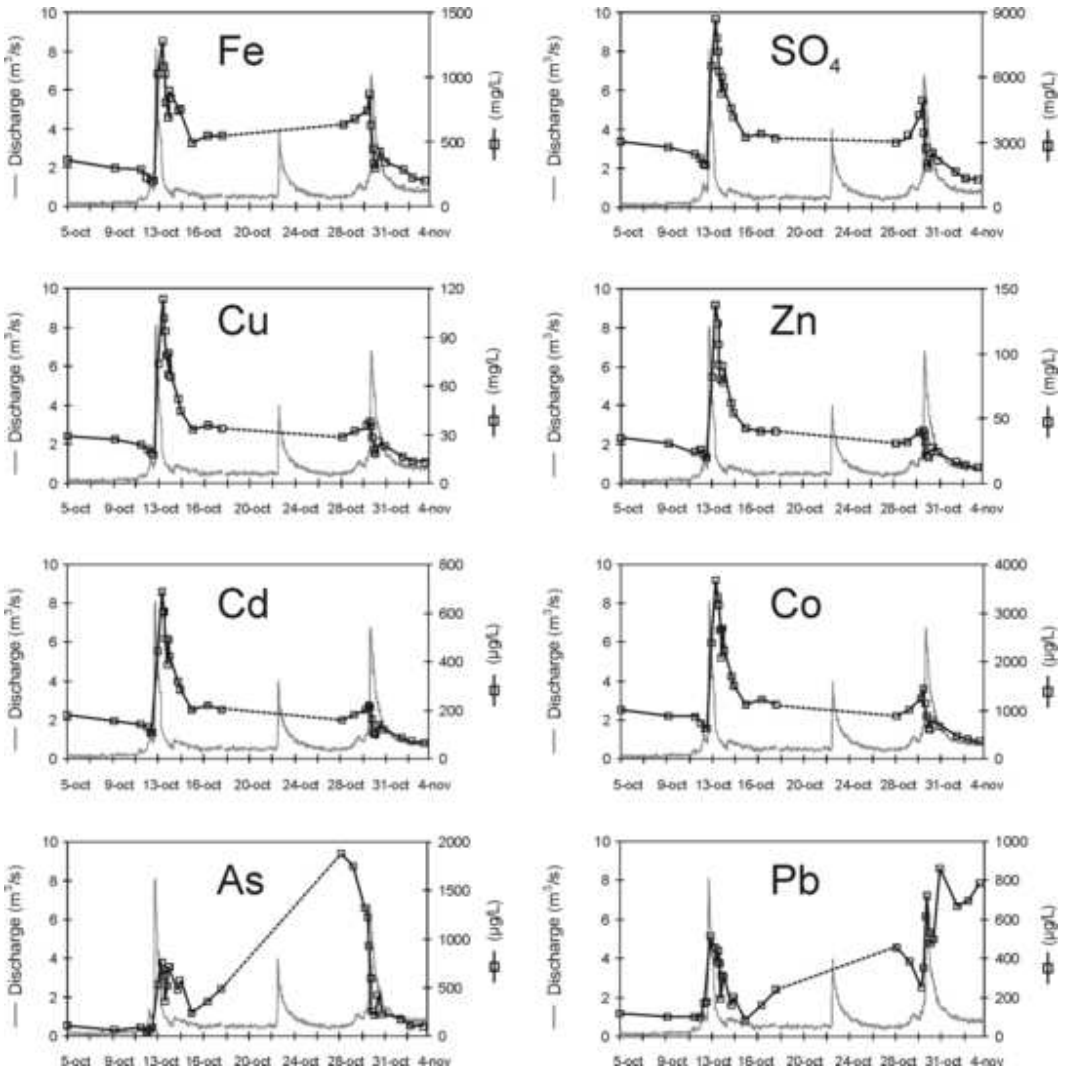

Figure 4. Evolution in concentration of some dissolved elements commonly found in sulfides.

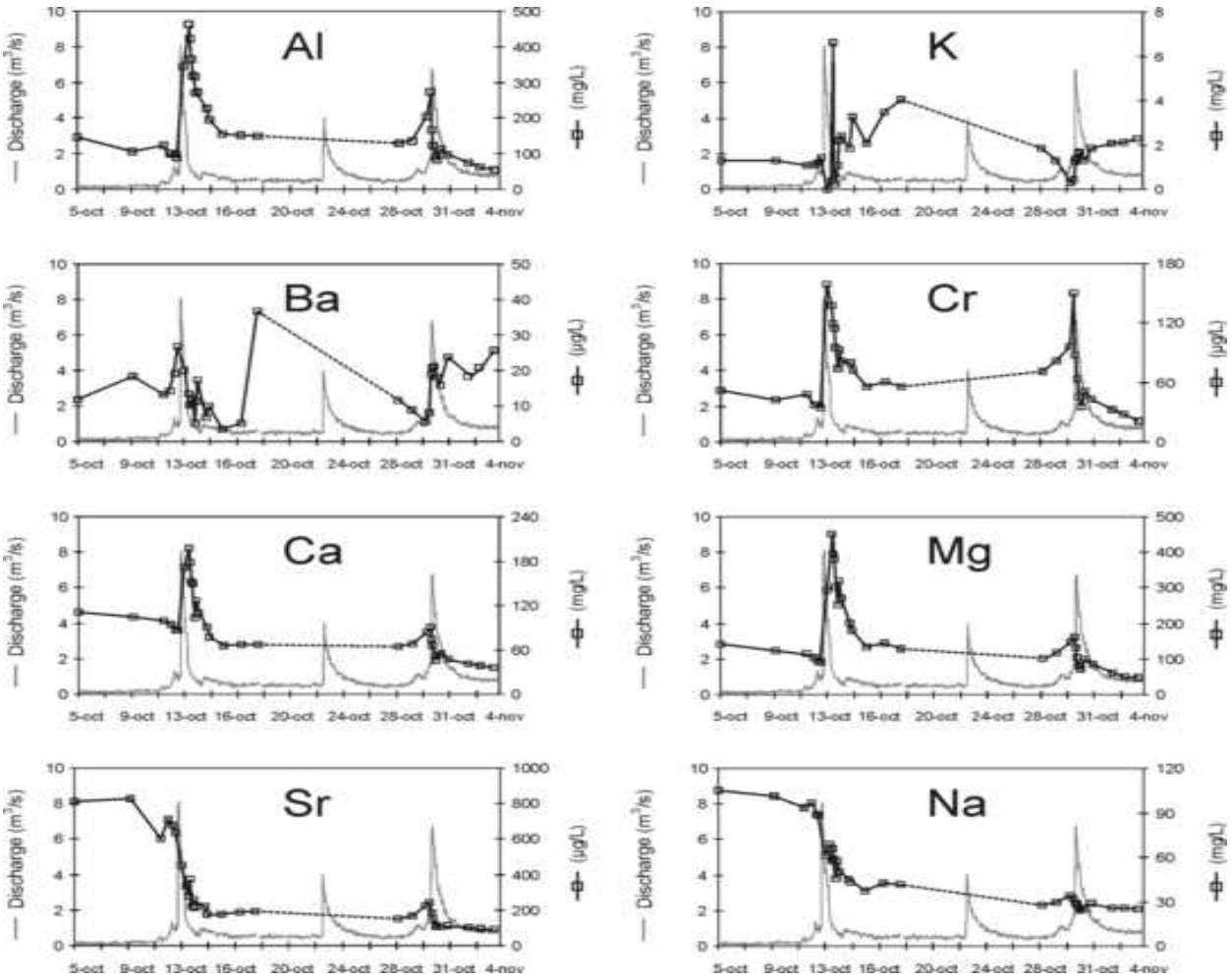

Figure 5. Evolution in concentration of some dissolved elements commonly found in alumino-silicate minerals.

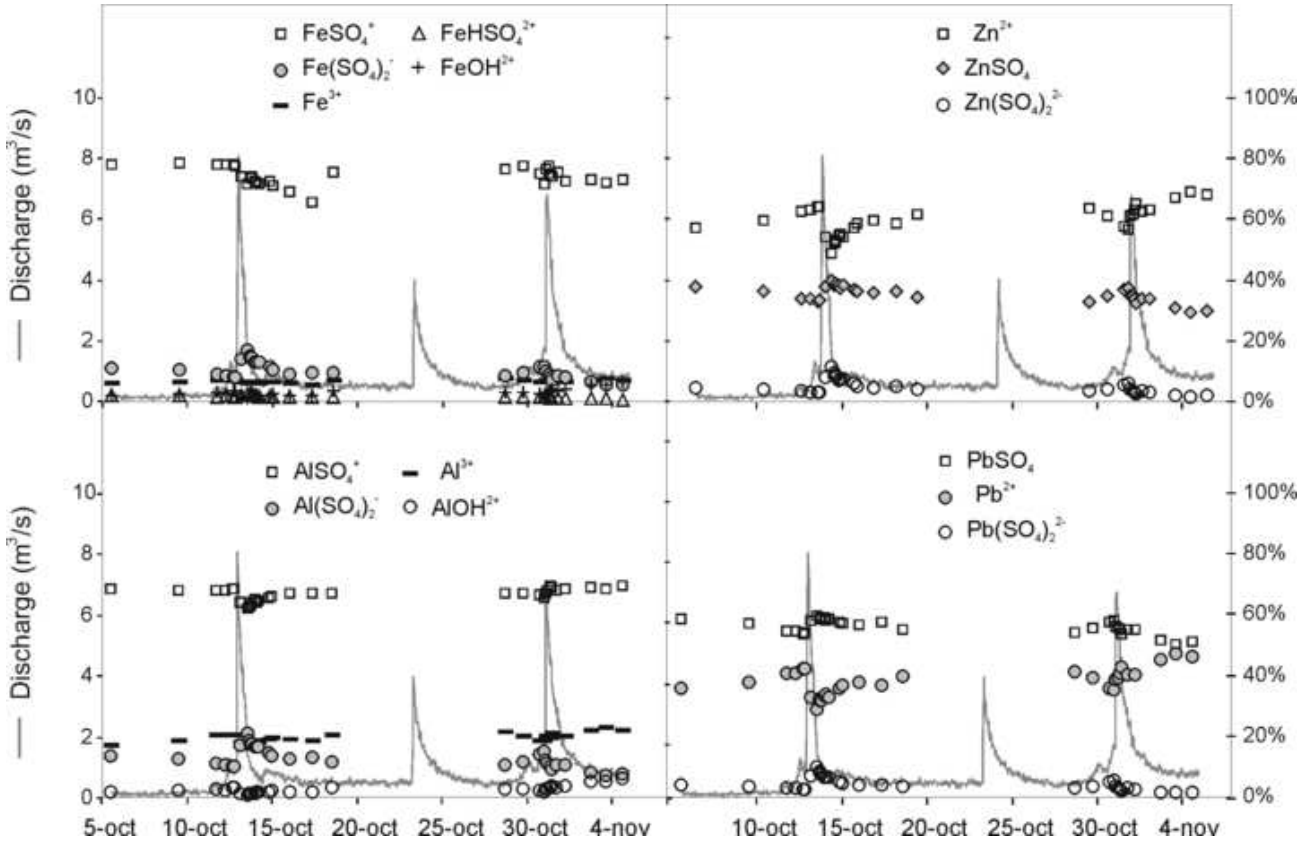

Figure 6. Evolution of main Fe, Al, Zn and Pb species during the monitored period.

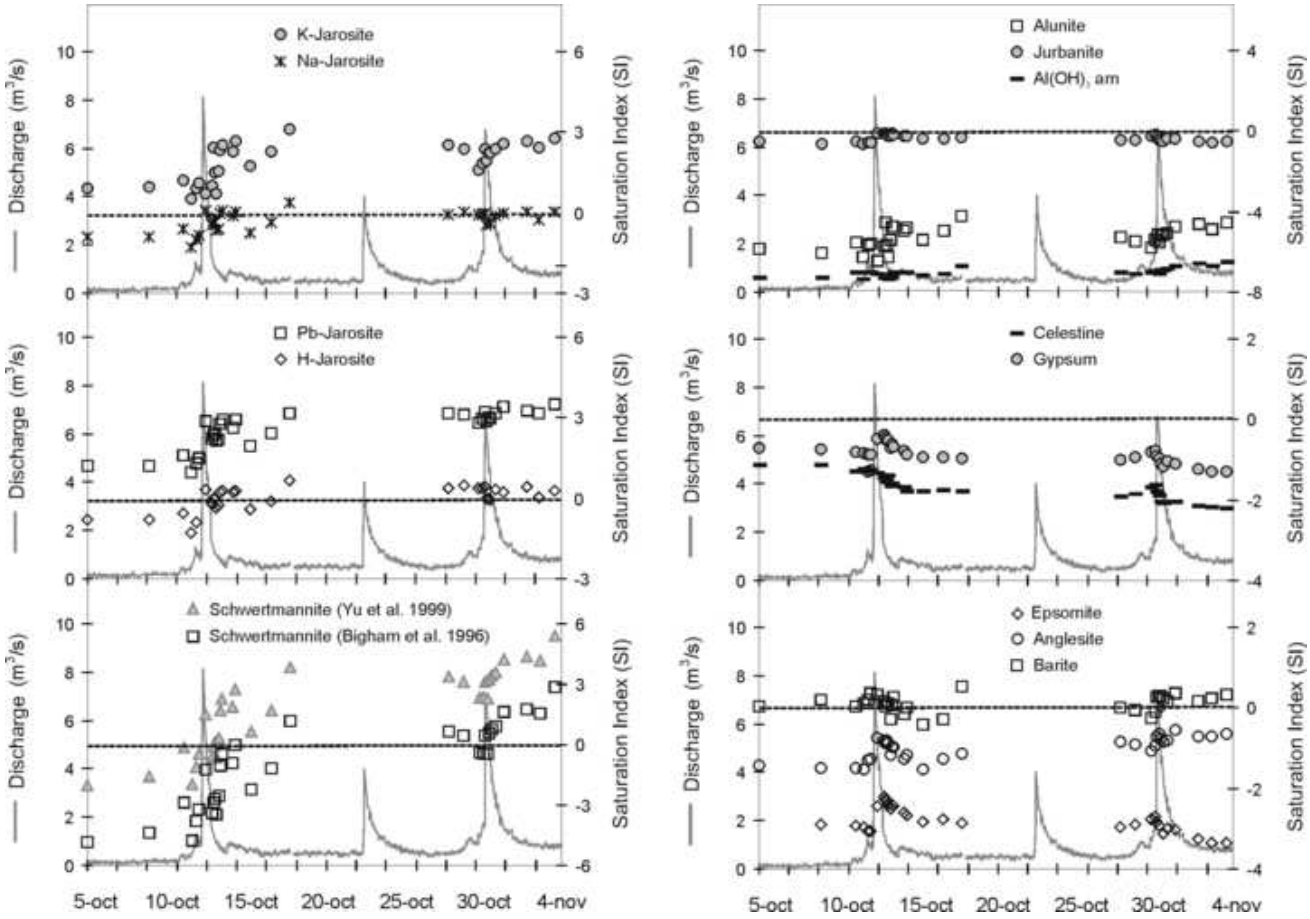

Figure 7. Evolution of saturation indices (SI) of most commonly-found minerals in AMD environments.

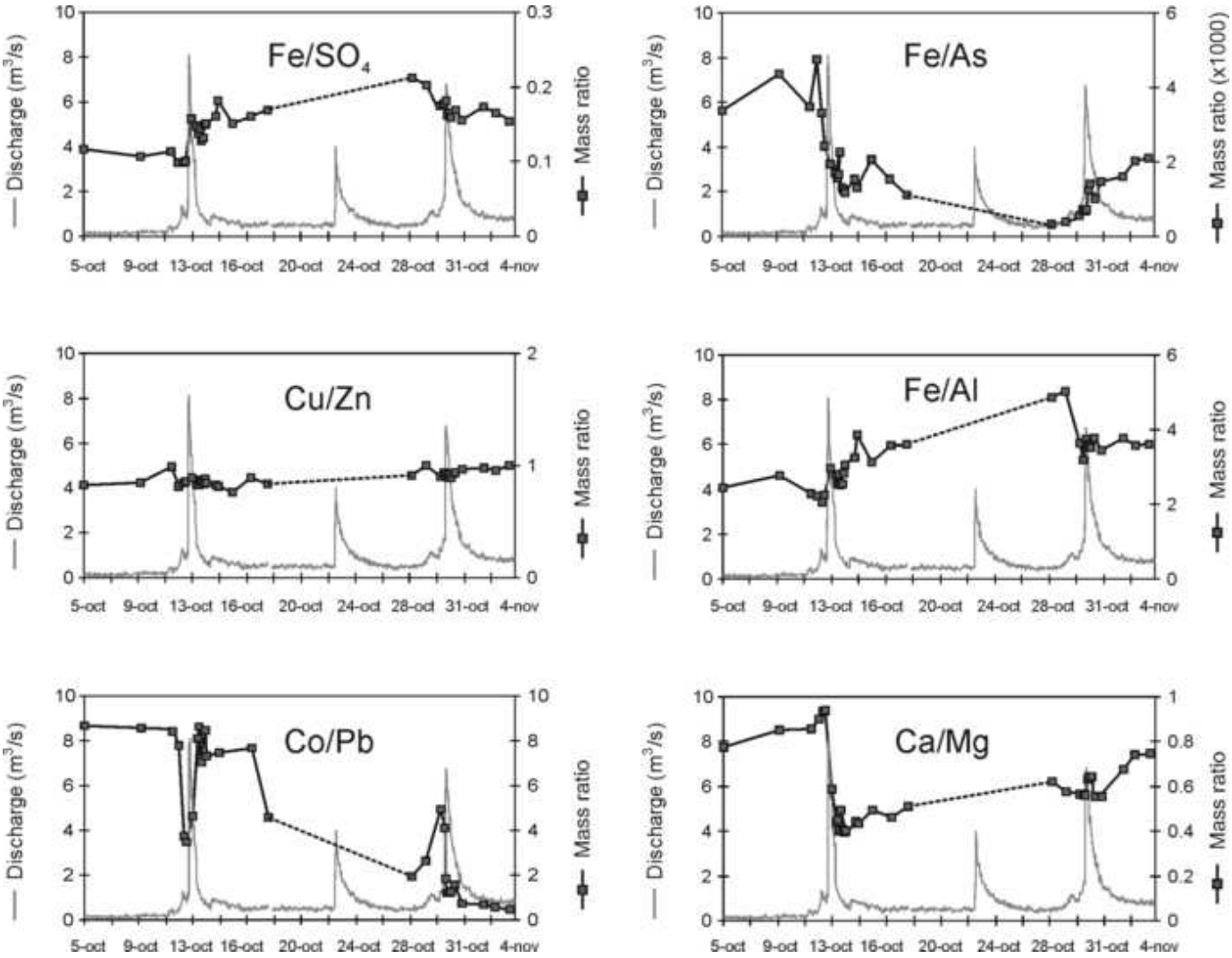

Figure 8. Evolution of some ionic ratios during the monitored period

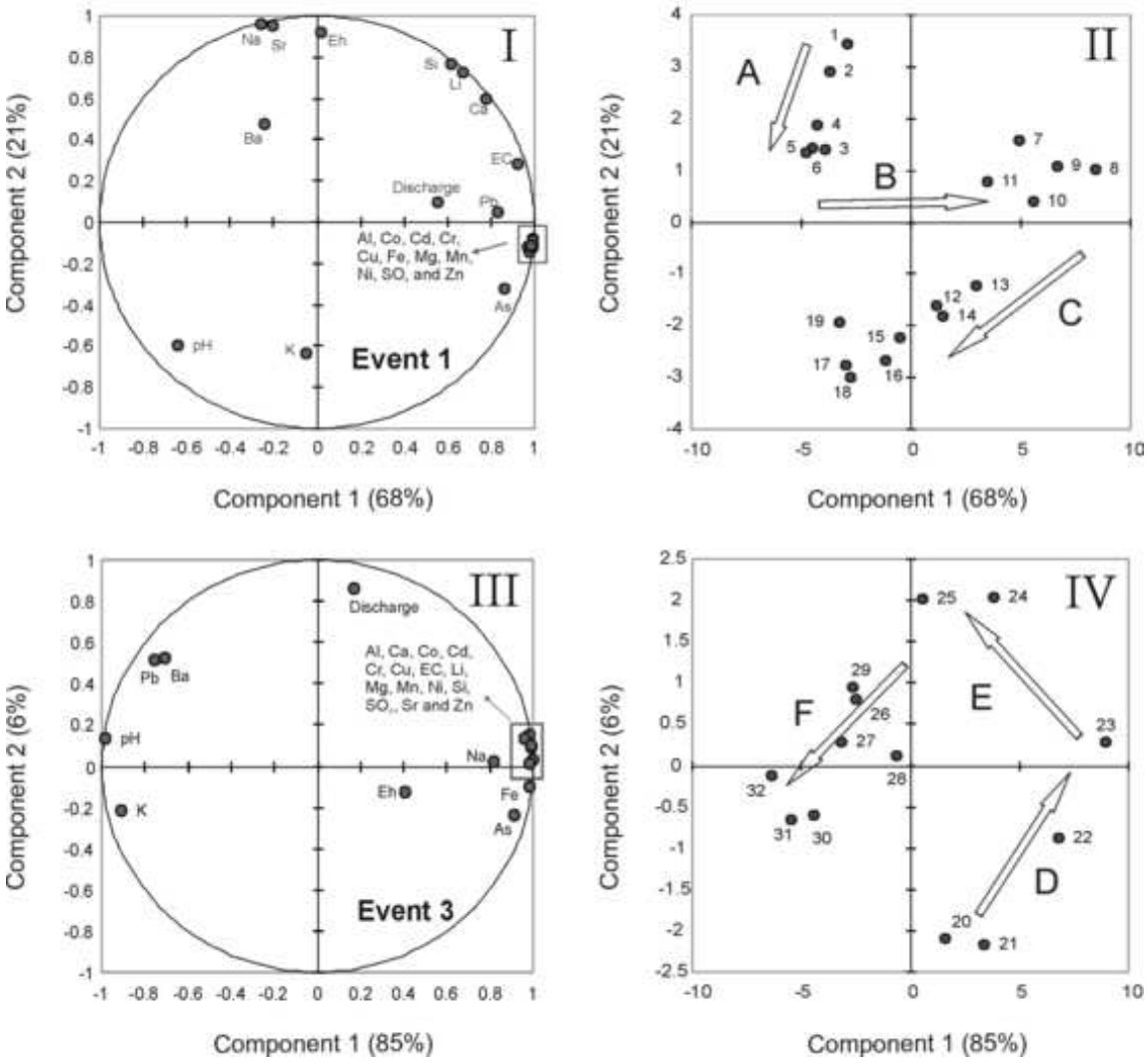

Figure 9. Results obtained from Principal Component Analysis (PCA) for Events 1 and 3.

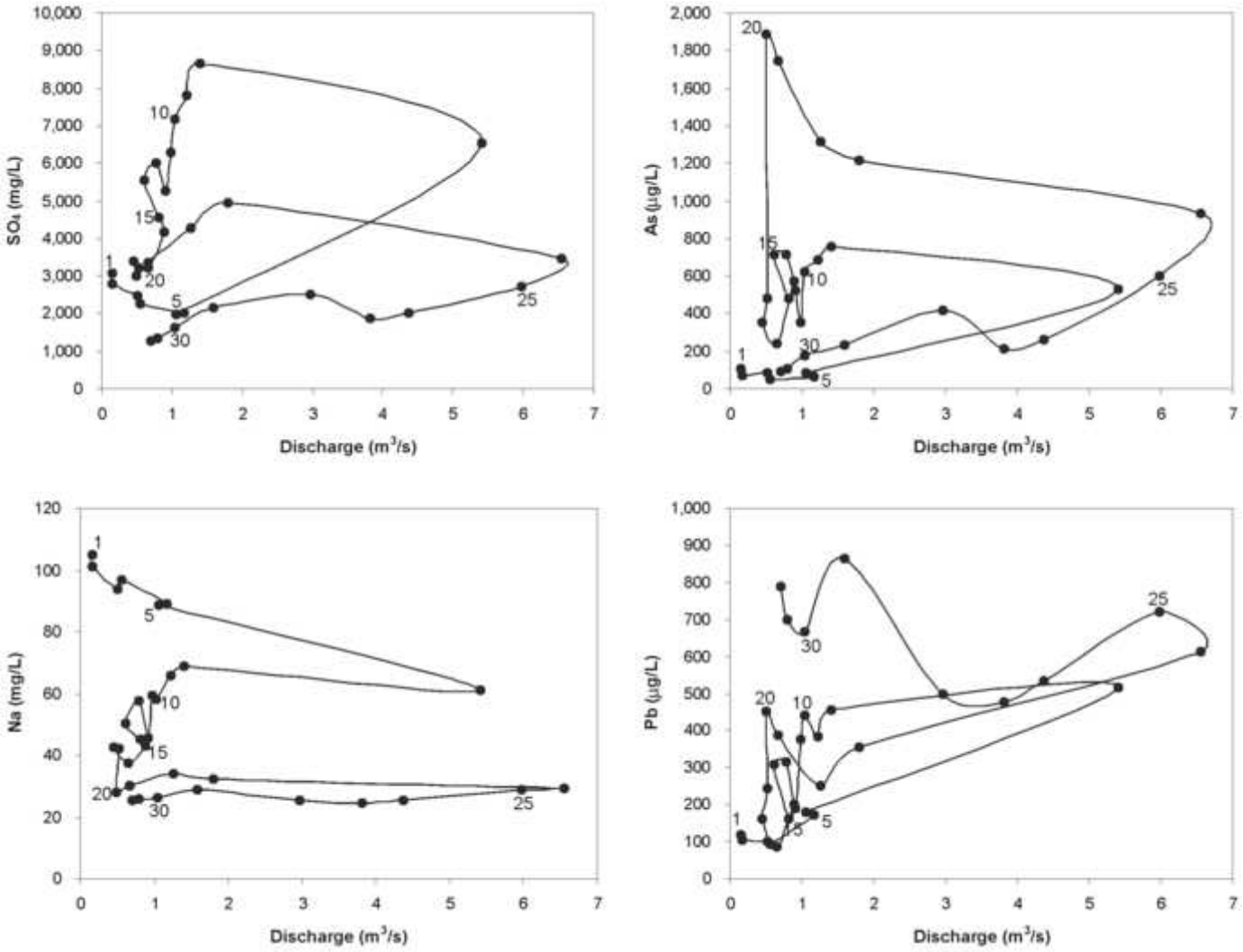

Figure 10. Discharge-Concentration (Q-C) relathionships for SO_4, As, Pb and Na. Numbers indicate sample codes.

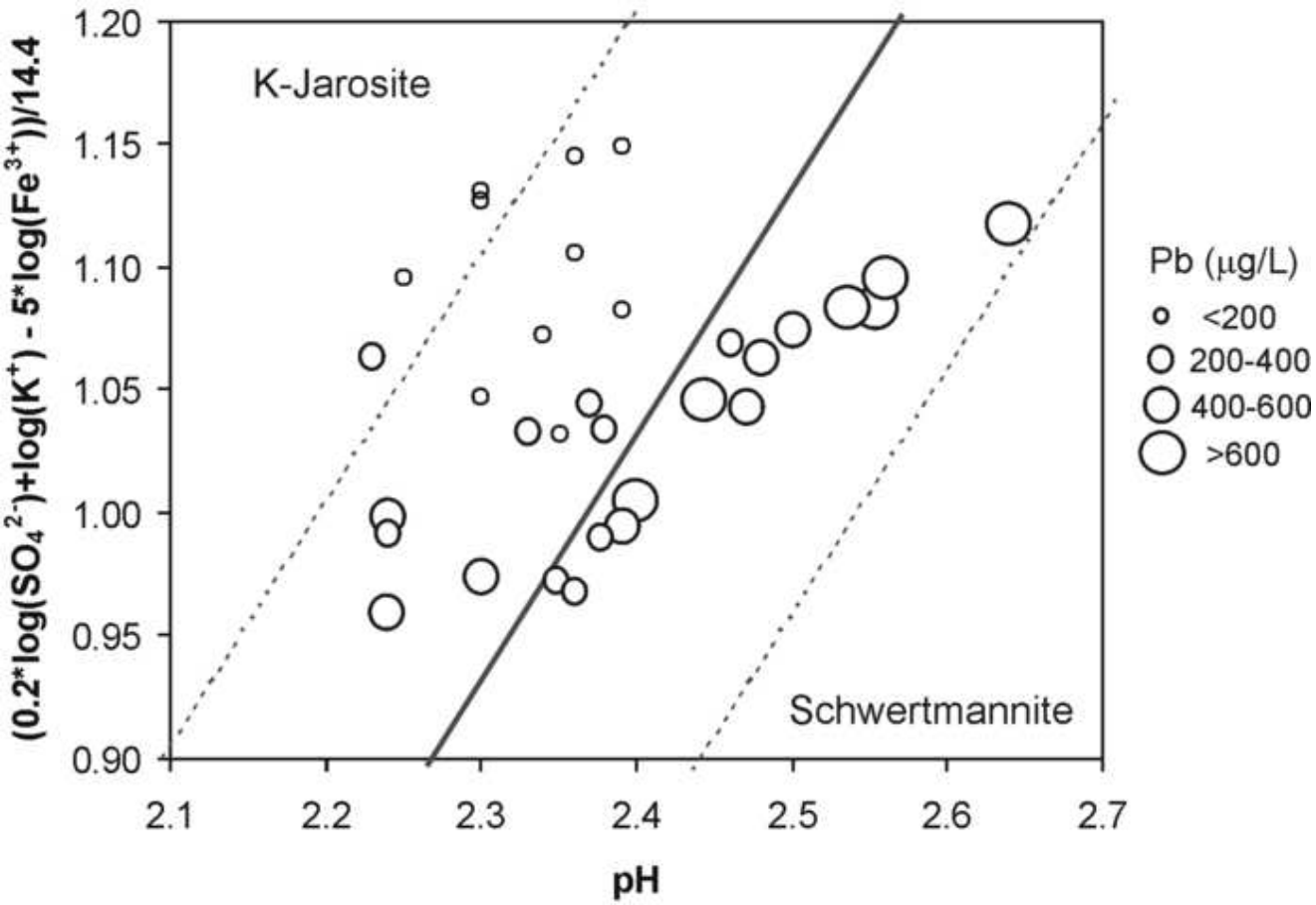

Figure 11. Stability fields for schwertmannite and K-jarosite and Pb concentration. The Ke used are those of Chapman et al. (1983) for K-jarosite and Yu et al. (1999) for schwertmannite. The dashed lines indicate the solubility of schwertmannite (log K_S = -10.5 ±2.5) proposed by Yu et al. (1999).

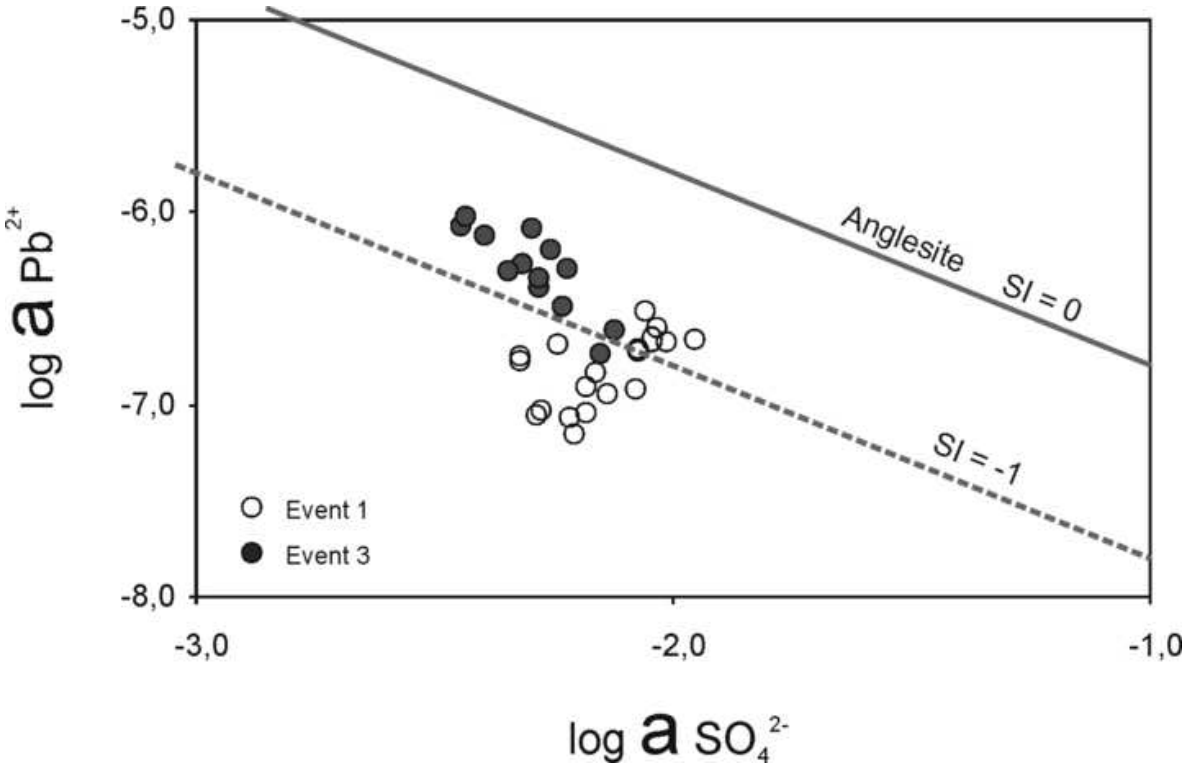

Figure 12. Relationship between SO_4^{2-} and Pb^{2+} activities.

Table captions

Parameter	Fe	Mg	Al	Na	Mn	Ca	Si	K	Zn	Cu	Co	Pb	Ni	Cr	Sr
	%								ppm						
Mean	16	2.0	2.2	0.65	0.26	0.10	<0.005	<0.01	7047	4677	196	123	43	18	11
Median	17	0.80	2.5	0.18	0.05	0.08	<0.005	<0.01	5240	4350	113	32	29	12	8.0
Minimum	0.32	0.10	0.31	0.04	0.03	0.01	0,22	<0.01	183	173	68	10	13	5.0	6.0
Maximum	29	6.4	4.6	3.4	0.66	0.29	13	0.46	17500	12200	419	1060	152	34	19
Percentile 25	6.9	0.26	1.0	0.16	0.05	0.04	<0.005	<0.01	4725	3470	82	14	24	10	7.0
Percentile 75	22	3.4	2.6	0.45	0.50	0.10	<0.005	<0.01	7053	4975	281	102	39	26	13

Table 1. Summary of composition of evaporitic sulfate salts precipitated in the Tinto catchment (modified from Cánovas et al., 2008).

		n	Average	Median	SD	C.V	Minimum	Maximum	Perc. 25	Perc. 75	D.L
Discharge	m^3/s	32	0.83	0.56	0.99	119%	0.05	8.13	0.42	0.89	
EC	mS/cm	32	4.49	4.25	1.5	33%	2.1	7.97	3.60	5.11	
pH		32	2.38	2.37	0.10	4.3%	2.2	2.64	2.30	2.45	
Acidity	mg $CaCO_3$/L	32	2794	2493	1408	50%	952	5663	1592	3745	
Eh	mV	32	791	782	36	4.6%	735	892	764	805	
Al	Main Elements (mg/L)	32	185	147	110	59%	55	462	100	271	0.08
Ca		32	91	85	42	46%	36	197	65	105	0.05
Cu		32	42	32	27	66%	13	113	23	55	0.10
Fe		32	574	545	300	52%	198	1280	298	766	0.11
K		32	1.8	1.4	1.3	71%	b.d.l	6.6	1.2	2.1	0.10
Mg		32	169	132	108	64%	48	451	98	216	0.05
Mn		32	23	18	14	62%	6.2	57	12	32	0.05
Na		32	50	43	26	51%	24	105	29	62	0.02
Sulphate		32	3782	3219	1973	52%	1281	8669	2239	5019	0.10
Si		32	25	21	13	54%	8.9	62	15	30	0.05
Zn		32	48	37	33	69%	13	137	24	66	0.15
As	Trace Elements (µg/L)	32	521	447	471	91%	47	1885	159	694	3.1
Ba		32	15	14	7.3	48%	3.6	37	10	19	1.0
Be		30	9.0	6.9	5.6	62%	b.d.l	24	5.0	13	1.1
Cd		32	250	191	172	69%	66	687	127	334	1.0
Co		32	1380	1065	913	66%	366	3674	717	1797	2.1
Cr		32	71	62	36	51%	21	159	43	89	1.9
Li		32	336	342	167	50%	95	697	210	448	1.6
Ni		32	559	427	340	61%	170	1431	318	756	1.3
Pb		32	372	365	221	59%	87	862	177	503	9.0
Se		30	93	74	60	64%	b.d.l	229	49	125	5.0
Sr		32	298	218	221	74%	90	828	152	346	2.1

Table 2. Summary of the results during the controlled period.

	Fe/SO_4	Cu/Zn	Fe/Al	Co/Pb	Fe/As	Ca/Mg	Na/SO_4	Sr/SO_4
Tinto waters								
Pre-event	0.12	0.83	2.4	8.7	3378	0.77	0.03	0.27
Peak Event 1	0.15	0.88	2.8	8.5	1252	0.39	0.01	0.04
Pre-event 3	0.21	0.91	4.9	2.0	336	0.62	0.01	0.05
End of Flood Events	0.15	1.00	3.6	0.47	2101	0.75	0.02	0.07
Evaporitic Salts								
Cánovas et al. (2008)	-	0.85	7.0	5.1	-	0.07	-	-
Buckby et al. (2003)	0.25	0.96	7.3	3.2	-	0.01	0.01	-
Hudson-Edwards et al. (1999)	-	-	-	-	111	-	-	-

Table 3. Ionic ratios of some elements in both evaporitic sulfate salts and Tinto river waters.

Load (t)	Al	As	Cd	Co	Cr	Cu	Fe	Li	Mn	Ni	Pb	SO_4	Zn
Flush out (First Event)	193	0.32	0.27	1.5	0.07	44	550	0.33	24	0.59	0.23	3754	52
Third Event	110	0.52	0.13	0.73	0.05	23	400	0.19	13	0.33	0.49	2323	25
Total event (a)	399	1.2	0.52	2.9	0.17	88	1278	0.68	48	1.2	1.1	8077	99
Total event (b)	372	-	0.50	2.8	-	83	-	0.68	51	1.1	-	7666	96
% annual (2005/06)	30%	29%	31%	29%	35%	27%	31%	-	27%	33%	22%	32%	28%
October 2004 [1]	420	0.41	0.49	3.3	0.10	100	770	0.58	71	1.0	6.8	5700	100
2005/06 [2]	1322	4.1	1.7	10	0.49	332	4094	-	175	3.6	5.1	25249	356

1. Cánovas *et al.* (2008)
2. Cánovas (2009)

(a) Calculated from Eq. 14

(b) Calculated from EC-concentration relationships

Table 4. Pollutant load (t) carried by the Tinto river during the controlled period.